Draft version November 18, 2025
Typeset using LaTeX twocolumn style in AASTeX7.0.1

Long-period transit searches should use a wider range of durations

Geert Jan Talens [1], Suzanne Aigrain [1], Luca Malavolta [2,3] and Leigh C. Smith [4]

[1] Denys Wilkinson Building, Department of Physics, University of Oxford, OX1 3RH, UK
[2] Dipartimento di Fisica e Astronomia "Galileo Galilei", Università di Padova, Vicolo dell'Osservatorio 3, I-35122 Padova, Italy
[3] INAF, Osservatorio Astronomico di Padova, Vicolo dell'Osservatorio 5, 35122 Padova, Italy
[4] Institute of Astronomy, University of Cambridge, Madingley Rd, Cambridge CB3 0HA, UK

ABSTRACT

We present a method for computing upper and lower limits to the expected duration of planetary transits given a range for the parameters of the host star, while explicitly accounting for non-zero impact parameter and eccentricity, and placing a basic constraint on the orbital stability through a minimum planet-star separation at periastron. We find that, especially at longer periods, the transit can be considerably shorter or longer than previous searches have assumed. No transits are known with such short or long transit durations, but it is unclear whether this is a real feature of the planet population or a combination of transit probability, observational bias, and detection bias.

Keywords: Transits (1711) — Exoplanets (498) — Exoplanet detection methods (489)

1. INTRODUCTION

Exoplanet transit searches are typically performed across a grid of transit durations, the limits of which are defined relative to a circular orbit and equatorial transit (A. Ofir 2014; M. Hippke & R. Heller 2019). In this note, we compute the longest and shortest transit durations expected as a function of orbital period for a given range of host star properties, while explicitly accounting for non-zero impact parameter and orbital eccentricity.

2. THE DURATION EQUATION

We start by combining equations 14 and 16 from J. N. Winn (2010) to obtain an expression for the full transit duration T_{14} for eccentric orbits:

$$T_{14} = \frac{P}{\pi}\frac{\sqrt{1-e^2}}{1+e\sin\omega}\sin^{-1}\left[\frac{R_\star}{a}\frac{\sqrt{(1+k)^2-b^2}}{\sin i}\right], \quad (1)$$

where P is the orbital period, $a/R_\star$ is the scaled semi-major axis, b is the impact parameter, $k = R_p/R_\star$ is the planet-star radius ratio, i is the orbital inclination, e is the eccentricity, and ω is the argument of periastron. For eccentric orbits, the impact parameter is given by:

$$b = \frac{a}{R_\star}\frac{1-e^2}{1+e\sin\omega}\cos i. \quad (2)$$

Equation 1 is an approximation, but more accurate expressions (e.g. D. M. Kipping 2008) are not required for our use case. Defining for convenience

$$\alpha = \frac{\sqrt{1-e^2}}{1+e\sin\omega}, \quad \beta = \frac{1-e^2}{1+e\sin\omega}$$

and using Eq. 2 to eliminate $\sin i$, Eq. 1 becomes:

$$T_{14} = \alpha\frac{P}{\pi}\sin^{-1}\left[\beta\sqrt{\frac{(1+k)^2-b^2}{\beta^2(a/R_\star)^2-b^2}}\right] \quad (3)$$

3. LIMITING PARAMETER VALUES

To compute the shortest and longest transit duration using Eq. 3, we first select limiting values for $a/R_\star$, k, b, e, and ω. The longest transits occur at apastron ($\omega = 270°$) for $b = 0$, while the longest occur at periastron ($\omega = 90°$) for high b. Transits become grazing for $b \geq 1-k$ and disappear entirely for $b \geq 1+k$. We choose a limiting value of $b = 0.9$, which covers $\sim 90\%$ of all cases while avoiding grazing transits for k up to 0.1. We consider planet sizes $0.01 \leq R_\mathrm{p}/R_\odot \leq 0.2$, i.e. approximately $1\,R_\oplus$–$2\,R_\mathrm{Jup}$ for a Sun-like star. If the properties of the star being considered is poorly constrained, appropriate radii at either end of the density range of interest should be used to convert R_p to k. The density range also controls the limiting values for $a/R_\star$ through Kepler's third law:

$$\left(\frac{a}{R_\star}\right)^3 \approx \rho_\star\frac{GP^2}{3\pi}. \quad (4)$$

Corresponding author: Geert Jan Talens
Email: geertjan.talens@physics.ox.ac.uk

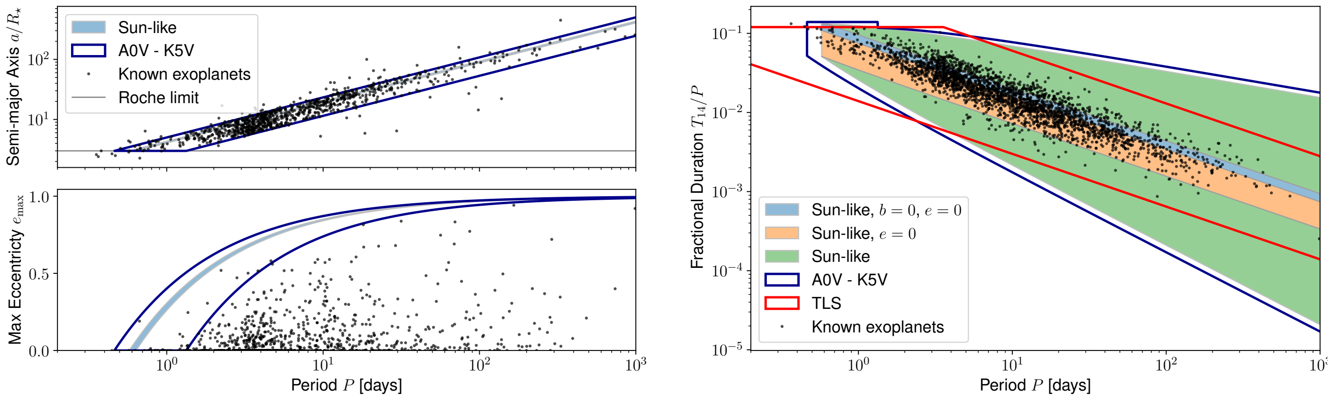

Figure 1. *Left:* Allowed range of semi-major axis (top) and maximum eccentricity (bottom) as a function of orbital period, for a Sun-like star with $\rho_\star = 1.26 - 1.54$ g/cm^3 (blue shaded area), and for A0V–K5V stars with $\rho_\star = 0.29$–2.38 g/cm^3 (dark blue lines). *Right:* Transit duration limits for a Sun-like star under different assumptions for impact parameter and eccentricity (blue, orange and green), and for the full A0V–K5V density range (dark blue line). The red line shows the limits as presented in M. Hippke & R. Heller (2019). In all panels, black points show known exoplanets with host star densities in the A0V–K5V range.

Following A. Ofir (2014), we assume that the orbit cannot enter the Roche limit of the host star, i.e., the minimum star-planet separation $d = a(1-e)$ must be $\geq 3R_\star$. This gives a maximum eccentricity $e_{\rm max} = 1 - 3R_\star/a$; the longest and shortest transits will occur at this limiting eccentricity.

Setting $a/R_\star = 3$ and using the stellar density range in Eq. 4 gives:

$$P_{\rm min} = 9\sqrt{\frac{\pi}{G\rho_{\star,\rm max}}}, \quad P_{\rm break} = 9\sqrt{\frac{\pi}{G\rho_{\star,\rm min}}}.$$

For $P > P_{\rm break}$ the entire density range produces valid orbits, but for $P_{\rm min} < P < P_{\rm break}$ the minimum density must be increased to keep $a/R_\star \geq 3$. In this period range we also use $R_{\star,\rm min}$ to convert R_p to k, slightly increasing the longest allowed durations.

In Fig. 1 the upper left panel shows the range of allowed $a/R_\star$ for A0 to K5 main sequence stars, with densities in the range $\rho_\star = 0.29 - 2.38$ g/cm^3 (M. V. Zombeck 1982). Also shown for comparison are known exoplanets (NASA Exoplanet Science Institute 2020, Otc. 22nd 2025) with host stars whose densities fall in that range. Some of the known planets fall outside the valid range of $a/R_\star$, we attribute this to measurement uncertainties and the fact that the planet parameters were compiled from multiple sources, which are not guaranteed to be mutually consistent. The lower left panel of Fig. 1 shows the maximum eccentricity for the limits on $a/R_\star$.

4. RESULTS

The right panel of Figure 1 shows the transit duration limits we obtain for Sun-like stars, first assuming equatorial transits and circular orbits and allowing only for the range of stellar density and star-planet radius ratio (blue shaded region), allowing for non-zero impact parameters (blue + orange), and also allowing for non-zero eccentricity (blue + orange + green). This clearly illustrates that eccentricity and impact parameter have a much larger impact on the range of allowed transit durations than the stellar density uncertainty.

The solid blue line shows the extended duration limits when considering A0V–K5V host stars. The small jump in the upper limit corresponds to $P_{\rm break}$. For comparison, we also show in red the duration limits implemented in the Transit Least Squares (TLS) code (M. Hippke & R. Heller 2019), and known transiting exoplanets with host star densities in the main sequence range as black points. Virtually all known planets fall within both the blue and red limits. It is unclear if the lack of planets with very short or long durations, which would only occur for eccentric orbits, is real, or reflects a detection bias. Systems with long orbital periods, high eccentricities and transiting close to periastron may have been missed by transit surveys, as the very short transits would have fallen outside the range of transit durations searched by most pipelines. The multi-day transits expected for long-period eccentric planets transiting close to apastron could have been missed for similar reasons. We therefore recommend searching long-baseline light-curves using these updated transit duration limits in the future. It should be noted, however, that other factors affect the detectability of very long-duration transits, including the detrending filters which are commonly applied to remove stellar variability (M. Hippke et al. 2019, and references therein), the difficulty of observing such transits from the ground, and the reduced transit probability of eccentric systems at apastron compared to equivalent systems on circular orbits (eccentric systems at periastron have increased transit probability).

ACKNOWLEDGEMENTS

This work has used the NASA Exoplanet Archive, which is operated by the California Institute of Technology, under contract with the National Aeronautics and Space Administration under the Exoplanet Exploration Program, and was supported by the UK Space Agency as part of its support for the UK component of the PLATO Mission.

REFERENCES

Hippke, M., David, T. J., Mulders, G. D., & Heller, R. 2019, AJ, 158, 143, doi: 10.3847/1538-3881/ab3984

Hippke, M., & Heller, R. 2019, A&A, 623, A39, doi: 10.1051/0004-6361/201834672

Kipping, D. M. 2008, MNRAS, 389, 1383, doi: 10.1111/j.1365-2966.2008.13658.x

NASA Exoplanet Science Institute. 2020, Planetary Systems Table, IPAC, doi: 10.26133/NEA12

Ofir, A. 2014, A&A, 561, A138, doi: 10.1051/0004-6361/201220860

Winn, J. N. 2010, in Exoplanets, ed. S. Seager (University of Arizona Press), 55–77, doi: 10.48550/arXiv.1001.2010

Zombeck, M. V. 1982, Handbook of space astronomy and astrophysics (Cambridge University Press)